Ecotoxicology and Environmental Safety 289 (2025) 117413

Contents lists available at ScienceDirect

Ecotoxicology and Environmental Safety

journal homepage: www.elsevier.com/locate/ecoenv

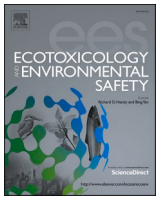

Dimethomorph induces heart and vascular developmental defects by disrupting thyroid hormone in zebrafish embryos

You Wei [a,b,1], Yunlong Meng [a,b,1], Kun Jia [b], Weijian Lu [a], Yushan Huang [c,*], Huiqiang Lu [a,**]

[a] Center for Clinical Medicine Research, First Affiliated Hospital of Gannan Medical University, Ganzhou, Jiangxi, China
[b] Center for drug Screening and Research, School of Geography and Environmental Engineering, Gannan Normal University, Ganzhou, Jiangxi 341000, China
[c] Center for Evidence Based Medical and Clinical Research, First Affiliated Hospital of Gannan Medical University, Ganzhou, China

ARTICLE INFO

Keywords:
Dimethomorph
Zebrafish
Thyroid follicles
Oxidative stress

ABSTRACT

Dimethomorph (DMT) is a widely-used selective active fungicide that effectively controls downy mildew, crown rot, and late blight in crops. The extensive application of DMT raises concerns about its ecological impact on non-target organisms in the environment. However, there is limited understanding of the toxicological properties of DMT on these organisms. In this study, we utilized zebrafish as an animal model to assess the toxicity of DMT induced by exposure 5.5–72 hours post-fertilization (hpf). During this period, we monitored and evaluated the development of the zebrafish heart and vascular system. Additionally, embryo samples were collected to perform molecular-level detection of PCNA, oxidative stress, and related genes. The results showed a concentration-dependent decrease in survival rate and hatching rate, shortened body length, slowed heart rate, and pericardial edema, body curvature and reduced eye size as DMT exposure concentration increased. Furthermore, DMT exposure led to impairments in the development of the heart, vascular, along with change in the expression levels of relevant genes. It also caused a decrease in cell proliferation and an increase in oxidative stress levels. Moreover, DMT disrupts the normal development of thyroid follicular cells, leading to a reduction in T3 levels. Thyroid hormone supplementation partially reverses the toxicity induced by DMT, increasing eye size, restoring body length, reducing spine curvature, and reducing pericardial edema. Therefore, we speculate that DMT likely affects the development of zebrafish embryos by disrupting normal thyroid follicle development.

1. Introduction

Current agricultural practices worldwide have extensively employed the use of pesticides as an effective method to maintain and improve crop productivity to meet the demands of a growing global population (Wang et al., 2017). However, the widespread utilization of pesticides has raised public concerns regarding their impact on the environment as well as on animal and human health (Kohler and Triebskorn, 2013; Munze et al., 2017; Yang et al., 2017). DMT (Dimethomorph) is an effective fungicide developed by BASF, Germany, for the prevention and control of oomycete diseases. It is particularly beneficial in controlling drug-resistant fields dominated by benzamide-resistant pathogens (Yang et al., 2021a; Liang et al., 2011; Liu et al., 2012).

With the widespread use of DMT, its residues have been detected in surface water (26.5 ng/L) (Navarro et al., 2024), soil (0.20–2.81 mg/kg) (Liu et al., 2012) and agricultural products such as peppers (0.05–1.28 mg/kg) (Liang et al., 2011), grapes (0.76±0.11 mg/kg) (Wang et al., 2018) and potatoes (0.0269–0.0391 mg/kg) (Chen et al., 2018). In addition, DMT has a long half-life in soil and can enter groundwater (Zambito Marsala et al., 2020). Current research on DMT primarily examines the residues and degradation rates of crops, soil in the environment, and other contact materials (Wang et al., 2018; Hengel and Shibamoto, 2000; Xu et al., 2015; Siegenthaler and Hansen, 2021; Baek et al., 2021). Among the 43 pesticide residues in Dendrobium officinale, DMT was found to have significant residues, with a concentration of 6.11 mg/kg (Xu et al., 2021). A skin exposure study of greenhouse planter workers demonstrated that DMT can be absorbed through the skin, despite the use of effective protective clothing by the

* Correspondence to: Center for Evidence Based Medical and Clinical Research, First Affiliated Hospital of Gannan Medical University, Ganzhou, Jiangxi 341000, China.
** Correspondence to: Center for Clinical Medicine Research, First Affiliated Hospital of Gannan Medical University, Ganzhou, Jiangxi 341000, China.
E-mail addresses: 3218680@qq.com (Y. Huang), luhq2@126.com (H. Lu).
[1] These authors contributed equally to this work.

https://doi.org/10.1016/j.ecoenv.2024.117413
Received 31 July 2024; Received in revised form 23 November 2024; Accepted 25 November 2024
Available online 18 December 2024

workers (Lesmes-Fabian and Binder, 2013).

DMT has the potential to infiltrate organisms and induce toxicity via environmental exposure, such as contaminated water, crops, or direct contact. DMT exhibits immunotoxicity in human Jurkat T cells; while DIM, as an androgen receptor antagonist, causes shortened anogenital distance in male rats; additionally, DIM leads to dose-dependent reductions in plasma corticosterone levels, affects ovarian gene expression, and impairs follicle growth in rats (Li et al., 2022; Scholze et al., 2020; Boberg et al., 2023). DMT induced oxidative stress may contribute to its toxicity (Wang et al., 2022; Fan et al., 2021a). DMT treatment of *P. parasitica* induced a significant accumulation of ROS (Hao et al., 2019), reflecting oxidative damage. Additionally, DMT exposure in soil resulted in oxidative stress in earthworms (Wang et al., 2017). In zebrafish embryos, exposure to DMT has been shown to significantly inhibit growth, delay hatching, suppress heart rate, and cause spinal curvature, pericardial edema, and yolk sac edema (Fan et al., 2021a; Yang et al., 2022a).

Despite these findings, the mechanisms underlying DMT induced toxicity remain poorly understood, particularly in relation to thyroid hormone function, which plays a crucial role in zebrafish development (Brown, 1997). Thyroid hormones, such as T3, are critical regulators of heart development, angiogenesis, and overall embryonic growth (Forhead and Fowden, 2014; Yen, 2001). Disruption of thyroid hormone signaling has been linked to developmental defects and oxidative stress, further implicating thyroid function in DMT-induced toxicity.

Zebrafish is not only a model organism, but also a test subject, widely used to detect the toxicity of chemical agents and contamination of soil and water (Bambino and Chu, 2017; Hill et al., 2005). It fills a scientific position between in vitro models and higher organisms (Horzmann and Freeman, 2018). Toxicity phenotypes in drug-exposed zebrafish and mammals share substantial similarities and can be used to study and model toxicity ranging from molecular initiation events to changes in biological health and behavior (Horzmann and Freeman, 2018).

The aim of this study was to assess the impact of DMT on embryonic development focusing on parameters such as survival rate, hatching rate, heart rate and body length, Additionally, we evaluated heart and angiogenesis development, along with the transcriptional effects of heart development-related genes (*gata4*, *nkx2.5*, *tbx5a*, *myh6*, *vmhc*, *nppa*), angiogenesis-related genes (*flt1*, *flt4*, *kdr*, *vegfa*). PCNA (Proliferating cell nuclear antigen) staining was performed to assess the proliferation of myocardial cells, alongside evaluating the transcription changes in proliferation-related genes (*ccnd1*, *ccne1*, *cdk2*, *cdk6*). We also measured key oxidative stress markers, including reactive oxygen species (ROS) level, catalase (CAT) activity and malondialdehyde (MDA) content, alongside assessing the transcription changes of antioxidant genes *hmox1a* and *nqo1*. Finally, given the key role of thyroid hormones in zebrafish development, this study explores whether T3 supplementation can alleviate DMT-induced developmental toxicity. This study provides valuable insights into the potential health risks posed by DMT to both aquatic life and humans.

2. Methods and materials

2.1. Zebrafish care and breeding condition

In this study, both AB wild-type and transgenic zebrafish lines were used, including *Tg(myl7:GFP)*, *Tg(fli:GFP)*, *Tg(tg:EGFP)*. All fish lines were obtained from the National Zebrafish Resource Center (Wuhan, China). Zebrafish were maintained in a recirculating water system at 28 ± 1 °C, with a 14-hour light and 10-hour dark cycle. The system provided continuous water flow. Zebrafish were fed newly hatched *Artemia* three times daily (morning, midday, and evening). For breeding, adult zebrafish were placed in spawning tanks in a 1:1 or 2:1 male-to-female ratio the evening before spawning, separated by baffles. The next morning, the baffles were removed, and embryos were collected two hours post-spawning. Embryos were cultured in E3 medium (5 mM NaCl, 0.17 mM KCl, 0.33 mM $CaCl_2$, 0.33 mM $MgSO_4$) with 0.00001 % Methylene Blue. Water parameters were controlled at a pH of 7.0 and conductivity of 450–550 μS/cm. Healthy embryos were selected for further experiments based on developmental stage and morphological criteria under a microscope.

2.2. Chemicals and reagents

DMT (CAS Number: 110488–70–5) was purchased from Shandong Renjie Biotechnology Co., Ltd. The primers used for this study were synthesized by Huada Gene Technology Co., Ltd. Additionally, three different kits were purchased from TransGen Biotech (Beijing, China): TransZol Up Enhanced RNA Extraction Kit, EasyScript One-Step gDNA Removal and cDNA Synthesis SuperMix Reverse Transcription Kit, and Real-Time Fluorescence Quantitation PerfectStart Green qPCR Super Mix Kit. Four reagents were obtained from Nanjing Jiancheng Bioengineering Institute (Nanjing, China): including the Total protein quantification kit (Coomassie brilliant blue method), CAT (catalase) visible light kit, micro-MDA (malondialdehyde) test kit, and ROS (reactive oxygen species) probe DCFH-DA. Thyroid hormones (T3/T4) supplied by MCE.

2.3. DMT exposure

A stock solution of DMT (1 g/L) was prepared by dissolving Dimethomorph in dimethyl sulfoxide (DMSO). After zebrafish spawning, 5.5 hpf embryos were handpicked under a microscope and transferred into a 6-well plate, with 15 embryos per well, and three biological replicates per group. The control group received embryo culture solution contained only 0.11 % DMSO (Ma et al., 2021; Zhong et al., 2021), while the treatment group was exposed to varying concentrations of DMT (0.7 mg/L, 0.9 mg/L, and 1.1 mg/L). DMT was diluted with embryo culture solution to achieve the desired concentration. Every 24 hours following administration, the water was replaced and the treatment duration lasted from 5.5 to 72 hpf. Fish were anesthetized with tricaine (0.16 g/L) and fixed in 1 % low-melting-point agarose for imaging. Images were taken using two microscopes: Leica M205 FA® (Leica, Germany) and Axio zoom V16® (Carl Zeiss, Germany).

At 72 hpf, zebrafish embryos post-DMT exposure were collected for subsequent experiments. All procedures followed the guidelines for the care and use of laboratory animals of the National Institute of Food and Drug Control of China.

2.4. Oxidative stress analysis

Zebrafish embryos were collected at 72 hpf after exposure to DMT for the analysis of oxidative stress-related biomarker expression. A total of 45 embryos per DMT dose were used for biomarker analysis of reactive oxygen species (ROS) levels, malondialdehyde (MDA) content, catalase (CAT) activity, and the expression changes of oxidative stress-related genes (*hmox1a* and *nqo1*). ROS levels, MDA content, and CAT activity were measured using standard commercial kits, following the manufacturer's protocols. Absorbance measurements were taken using a multifunctional microplate reader (PerkinElmer Victor Nivo, USA), and enzyme activity was calculated based on the formulas provided in the reagent kits. ROS-staining images were captured using a Leica microscope (Leica M205 FA®, Leica, Germany), and fluorescence intensity was quantified using ImageJ software (National Institute of Health, USA). For ROS staining analysis, 15 embryos were used per DMT concentration.

2.5. Histological preparation and staining

Zebrafish embryos (72 hpf) were fixed overnight with 4 % paraformaldehyde (PFA) at 4°C, with 15 embryos per DMT exposure concentration. Following fixation, the embryos were then washed three

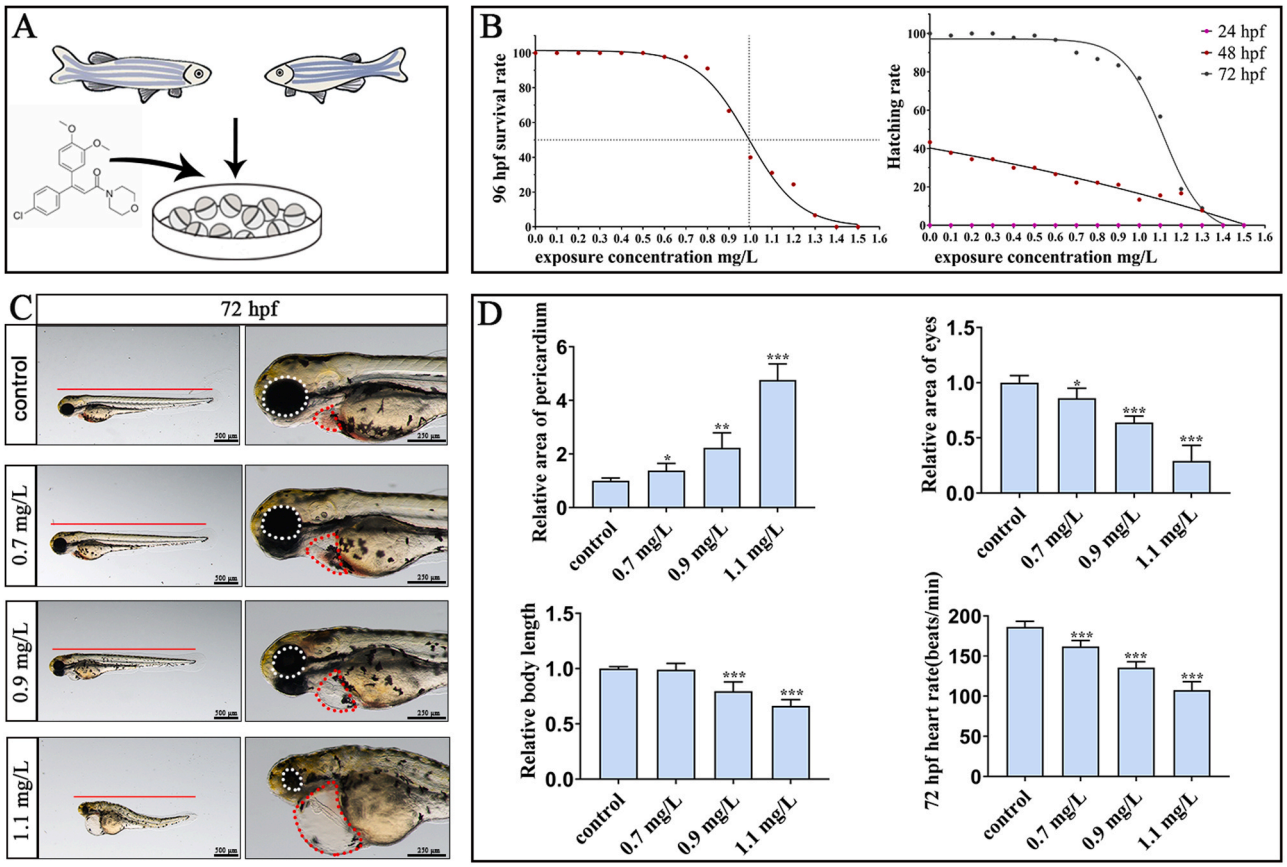

Fig. 1. DMT exposure induces acute toxicity and developmental defects in zebrafish embryos. (A) Schematic diagram and molecular structure of DMT exposure experiment. (B) Effect of different concentrations of DMT on the survival rate of zebrafish embryos at 96 hpf and on the hatchability statistics of zebrafish embryos. (C) The phenotype of developmental defects caused by DMT exposure was observed under the bright field of a microscope. (D) Statistics of changes in heart rate, eye area, body length and pericardial area of zebrafish embryos. Red dashed area indicates the pericardium.; White dashed area indicates the eye. The asterisk sign indicates significant differences between DMT treatment and negative control (*p<0.05, **p<0.01, ***p<0.001).

times in 70 % ethanol, with each wash lasting five minutes. The embryos were then dehydrated through a graded ethanol series (80 %, 90 %, 95 %, and 100 %). After dehydration, the samples were immersed in a xylene/ethanol mixture (1:1) for 20 minutes, followed by xylene for 50 minutes, xylene/paraffin (1:1) for 60 minutes, and finally paraffin for 90 minutes, with the paraffin replaced twice during this period. The samples were then cooled for solidification. After paraffin embedding, wax trimming, sectioning, and slide preparation were performed. Hematoxylin-eosin (HE) staining was conducted according to standard procedures as previously described (Wang et al., 2019; Xiong et al., 2019a).

2.6. PCNA immunostaining

A total of 15 embryos were collected from both the control group and the group exposed to 1.1 mg/L DMT. After collection, embryos were rinsed three times with embryo water, with each wash lasting five minutes. The embryos were then fixed overnight in 4 % paraformaldehyde (PFA) at 4°C. The next day, embryos were washed three times with PBS for five minutes each and blocked using PBTN (PBS + 1 % Triton X-100 + 4 % Bovine Serum Albumin + 0.02 % NaN3) for two hours at 4°C. Following blocking, the embryos were incubated with Anti-PCNA (Proliferating Cell Nuclear Antigen) antibody (1 μL antibody diluted in 1 mL PBTN) at 4°C overnight. After incubation, the embryos were washed five times with PT solution, with each wash lasting 45 minutes. They were then incubated with the secondary antibody (mouse anti-638) diluted with 1 mL PBTN (1 μL secondary antibody) and protected from light overnight at 4°C. The next day, the secondary antibody was removed, and the embryos were washed five times with PT solution (45 minutes per wash). Finally, images were captured using a confocal microscope (Leica TCS SP8), following the detailed operational steps as described in previous literature (Xiong et al., 2019a).

2.7. RNA extraction and qPCR analysis

72 hpf after DMT exposure, total RNA was extracted from all treated embryos (100 embryos per group). RNA extraction and reverse transcription reaction were performed according to the protocols provided by the commercial kits and as described in previous literature (Xiong et al., 2019b). Quantitative real-time polymerase chain reaction (qPCR) was performed using the ABI Step-One + RT-PCR® system [Applied Biosystem, CA, USA]. Gene expression was quantitatively analyzed, normalized to β-actin as the internal control. The data were presented as 2-ΔΔCt, and the primer sequences are provided in Supplementary Table S1.

2.8. Detecting T3 levels in zebrafish embryos

At 72 hpf, we collected 30 embryos from both the control group and the 1.1 mg/L DMT-treated group. The embryos were homogenized in 300 μL of physiological saline, centrifuged at 3000×g for 10 minutes, and the supernatant was collected for T3 level measurement. The T3 ELISA kit (purchased from Shanghai Keshun Biotechnology Co., Ltd.) was used according to the manufacturer's instructions provided in the manual.

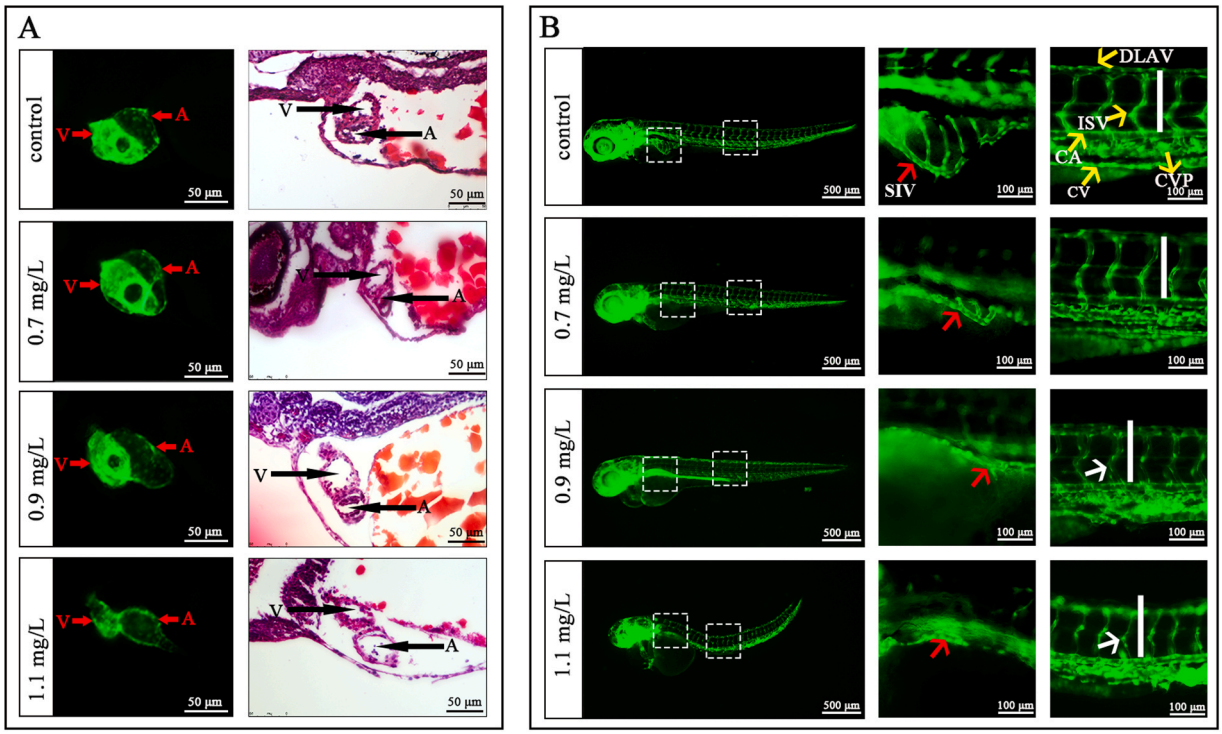

Fig. 2. DMT exposure induces defects in embryonic heart and vascular development. (A) After DMT was exposed to the transgenic fish strain *Tg(myl7: EGFP)*, fluorescence images were taken; and Staining of heart tissue sections. (B) After DMT was exposed to the transgenic fish strain *Tg(fli:GFP)*, fluorescence images were taken. Arrows indicate the atria and ventricles. A: atrium; V: ventricle; SIV: sub-intestinal venous; DLAV: dorsal longitudinal anastomotic vessel; ISV: intersegmental vessel; CVP: caudal vein plexus; CV: caudal vein.

2.9. Rescued experiment

A rescue experiment was conducted on the group treated with the highest concentration of DMT (1.1 mg/L). Embryos treated with embryo culture solution served as negative control. T3 and T4 [MCE, UV ≥ 99.98 %] were added to the 1.1 mg/L DMT exposure group at final concentrations of 2 μM each. At 72 hpf, images were captured using a Leica M205FA® [Leica, Germany].

2.10. Statistical analysis

All experimental data were analyzed using GraphPad Prism 8.0, Microsoft Excel 2019, Photoshop, and ImageJ. ImageJ was used to analyze area, body length, and fluorescence intensity measurements. Bar graphs were generated using GraphPad Prism 8.0, and a logistic regression analysis was conducted to calculate the DMT lethal concentration 50 (LC50). In Microsoft Excel 2019, Student's t-test was applied to assess differences between groups. Data are presented as mean ± standard deviation (SD). Statistical significance between the dimethomorph-treated group and the negative control was indicated by asterisks in the figures, with the following thresholds: *$p < 0.05$, **$p < 0.01$, ***$p < 0.001$. Photoshop was used for figure layout and formatting.

3. Results

3.1. DMT induced morphological deformities

To evaluate the bio-toxicity of DMT on early zebrafish embryos, we conducted a pre-experimental treatment using exposure concentrations ranging from 0 mg/L to 1.6 mg/L, with a concentration gradient of 0.1 mg/L. The exposure mode and the molecular structural of DMT are depicted in Fig. 1A. As shown in Fig. 1B, embryo death began at a DMT concentration of 0.8 mg/L, and mortality reached 100 % at 1.4 mg/L, with an LC_{50} of approximately 1.0 mg/L. The hatching rate is a crucial indicator of the toxicity of compounds on zebrafish embryo development. Based on the experimental data, DMT exposure significantly inhibited normal hatching, A DMT concentration of 0.7 mg/L reduced the hatching rat, with 50 % of the hatching rate occurring between 1.1 and 1.2 mg/L.

As shown in Fig. 1C, zebrafish embryos were exposed to DMT concentrations of 0 mg/L, 0.7 mg/L, 0.9 mg/L, and 1.1 mg/L from 5.5 to 72 hpf. Statistical analyses were performed on relevant indicators, as presented in Fig. 1D. At 0.9 mg/L DMT, significant developmental changes were observed: the eye area decreased, atrioventricular spacing increased, and the pericardium and yolk areas expanded considerably. Additionally, zebrafish body length was reduced, and the embryos exhibits a curved shape. Hheart rate also decreased in a concentration-dependent manner. with the most pronounced effects observed at 1.1 mg/L. In summary, the exposure of zebrafish embryos to DMT resulted in developmental toxicity.

3.2. Heart and vascular developmental defects

The heart is one of the first functional organs to develop in zebrafish and is highly susceptible to environmental toxins and drug exposure. After DMT exposure, we observed significant cardiac abnormalities, including an increased atrioventricular spacing, an enlarged pericardium, and a reduced heart rate, which indicated a direct impact on the heart. To further investigate the effects of DMT on zebrafish embryonic heart development, we utilized the transgenic line *Tg (myl7:EGFP)* to monitor cardiac developmental. Our results revealed that DMT exposure caused an elongation in the distance between the atrium and ventricle. Additionally, and histological sections of the heart tissue indicated a concentration-dependent reduction in cardiomyocytes (Fig. 2A).

Angiogenesis plays a critical role during zebrafish embryo development (Lee et al., 2021a). To investigate the potential impact of DMT exposure on this process. We conducted exposure experiments using a

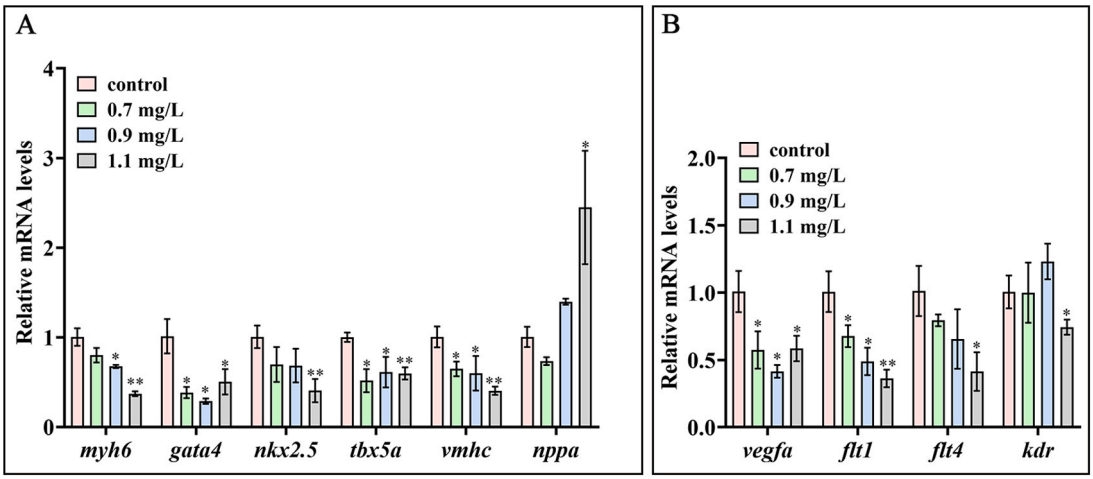

Fig. 3. Transcriptional changes in related genes. (A) Expression of zebrafish embryo heart development-related genes (*gata4*, *nppa*, *myh6*, *tbx5a*, *nkx2.5*, *vmhc*) after exposure to DMT. (B) Expression of zebrafish embryo vascular development-related genes (*vegfa*, *flt1*, *flt4*, *kdr*) after exposure to DMT. The asterisk sign indicates significant differences between DMT treatment and negative control (*p<0.05, **p<0.01, ***p<0.001).

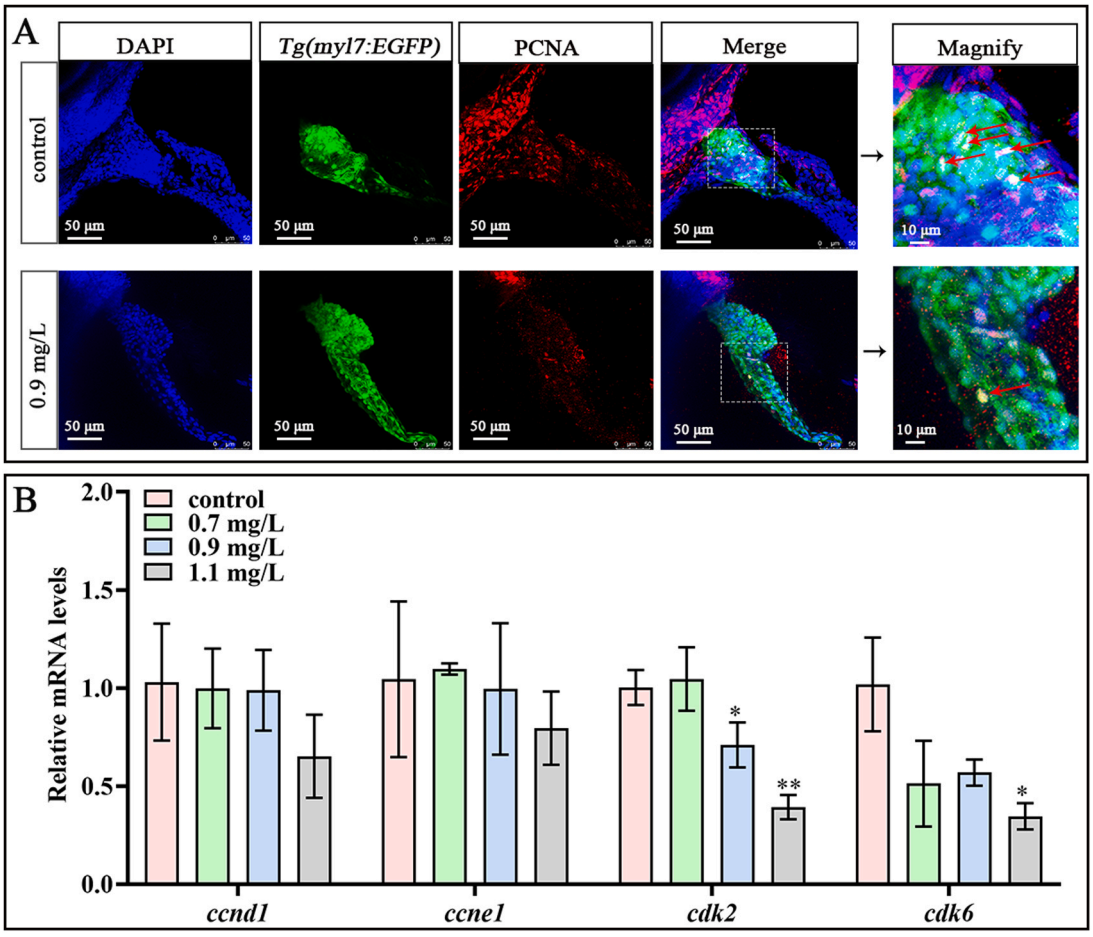

Fig. 4. Effects of DMT exposure on cell proliferation. (A) PCNA antibody staining detects the proliferation of zebrafish embryonic cardiomyocytes exposed to different concentrations of DMT at 72 hpf. (B) Expression of zebrafish embryo cell proliferation-related genes (*ccnd1*, *cdk6*, *ccne1*, *cdk2*) after exposure to DMT. The asterisk sign indicates significant differences between DMT treatment and negative control (*p<0.05, **p<0.01, ***p<0.001).

transgenic fish line *Tg (fli:GFP)*, which expresses green fluorescence to label vascular structures. As shown in Fig. 2A, increasing concentrations of DMT exposure led to the inhibition of sub-intestinal venous (SIV) development in zebrafish embryos, with a clear concentration-dependent effect (indicated by red arrows). The length of the intersegmental vessels (ISV) was reduced, and defects in their shape were observed. Additionally, the formation of dorsal longitudinal anastomotic vessel (DLAV), caudal vein plexus (CVP), and caudal vein (CV) was impaired, with CV being absent in the highest exposure group. Interestingly, The caudal artery (CA) does not seem to be impacted.

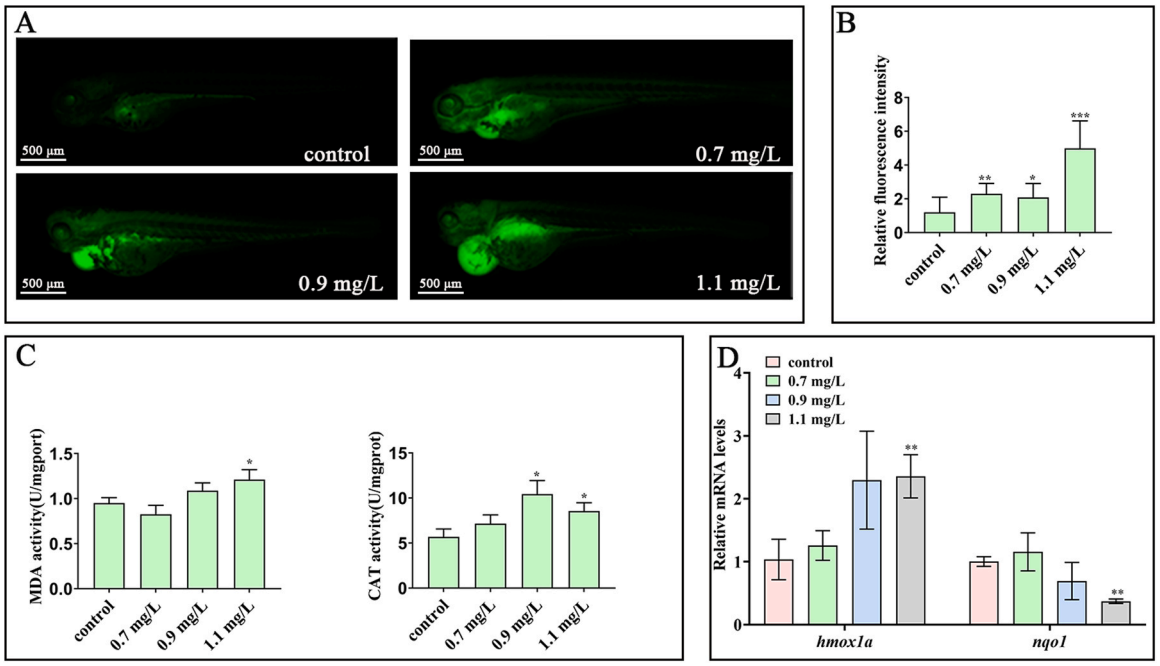

Fig. 5. DMT induces oxidative stress in zebrafish embryos. (A) Distribution of fluorescence visualizing ROS in zebrafish larvae exposed to different concentrations of DMT. (B) Fluorescence intensity of ROS after exposure to different concentrations of DMT. (C) MDA and CAT activities after exposure to different concentrations of DMT. (D) Expression of zebrafish embryo oxidative stress-related genes after exposure to DMT. The asterisk sign indicates significant differences between DMT treatment and negative control (*p<0.05, **p<0.01, ***p<0.001).

3.3. Expression of heart and vascular-related genes

Heart development is a continuous and highly intricate process, during which transcription factors, as well as growth and differentiation factor, play crucial roles in regulating the precise formation and function of cardiac tissues. As a result, we analyzed the transcriptional expression of genes associated with zebrafish heart development (Fig. 3A). Our results revealed a significant decrease in the expression of *gata4* and *tbx5a*. The expression of *nkx2.5* was markedly suppressed at the highest DMT exposure concentration of 1.1 mg/L. The expression of heart-specific gene *myh6* and *vmhc* showed a concentration-dependent decrease, while *nppa* expression significantly increased at a concentration of 1.1 mg/L. Therefore, exposure to DMT induces developmental malformations in the heart and disrupts the normal expression of genes associated with cardiac development. Furthermore, we assessed the effects of DMT on the transcriptional activities of angiogenesis-associated genes (*flt1*, *flt4*, *vegfc*, and *kdrl*). The results are presented in Fig. 3B, and demonstrating that the mRNA expressions of *flt1*, *flt4* and *vegfa* were significantly down-regulated following DMT exposure. However, no significant change was observed in transcription level of *kdr*. In conclusion, DMT disrupts the expression of angiogenesis-related genes, leading to abnormalities in angiogenesis.

3.4. Effects of DMT exposure on cell proliferation

To evaluate the effect of DMT exposure on cell proliferation, we selected embryos that were exposed to 1.1 mg/L of DMT for PCNA staining experiments. PCNA (Proliferating Cell Nuclear Antigen) plays a crucial role in the initiation of cell proliferation and is widely used as a marker to assess cell proliferation status. The results show that exposure to DMT reduces the number of PCNA-positive cells, indicating a decrease in the proliferation of zebrafish cardiomyocytes (Fig. 4A). Additionally, we evaluate the variations in the expression of cell proliferation-related genes in zebrafish. The results are shown in Fig. 4B, demonstrating that *cyclin D1* (*ccnd1*) and cyclin E1 (*ccne1*) expressions were slightly reduced, though the differences were not statistically significant compared to the control group. However, as DMT exposure increased, a marked downregulation of *cdk2* mRNA was observed at 0.9 mg/L and 1.1 mg/L. Furthermore, the expression of cyclin-dependent kinase 6 (*cdk6*) significantly reduced at 1.1 mg/L. In summary, DMT exposure led to the downregulation of key genes involved in cell proliferation. Combined with cardiomyocyte proliferation experiment, we speculated that DMT may induce the decrease of cell proliferation during zebrafish embryo development.

3.5. DMT induces increased levels of oxidative stress

Increases in oxidative stress levels are crucial biological indicators for assessing aquatic toxicology, as exposure to chemical toxicants elevates reactive oxygen species (ROS) levels, leading to disruption of the endogenous redox balance. As shown in Fig. 5A, the intensity of green fluorescence as the exposure concentration of DMT rose, indicating a persistent accumulation of reactive oxygen species (ROS). The ROS accumulation was predominantly observed in the heart and surrounding areas, which showed the brightest fluorescence signal, suggesting that oxidative stress was most prominent in these regions. The statistical analysis presented in Fig. 5B indicates a positive correlation between the intensity of ROS fluorescence and increasing DMT exposure concentrations, Additionally, as shown in Fig. 5C, elevated concentrations of DMT led to a significant increase in malondialdehyde (MDA) content and catalase (CAT) enzyme activity. Moreover, Fig. 5D demonstrates that DMT exposure significantly up-regulated the oxidative stress-related gene *hmox1a*, while *nqo1* expression was significantly down-regulated. In conclusion, the study indicates that DMT exposure induces oxidative stress and alters gene expression levels in embryos, which may lead to the observed developmental defects in zebrafish embryos.

3.6. Rescue experiment

Thyroid hormones are among the key hormonal regulators of antioxidant balance (Mancini et al., 2016). Additionally, their impact on heart contractility, heart rhythm, and vascular function has been well

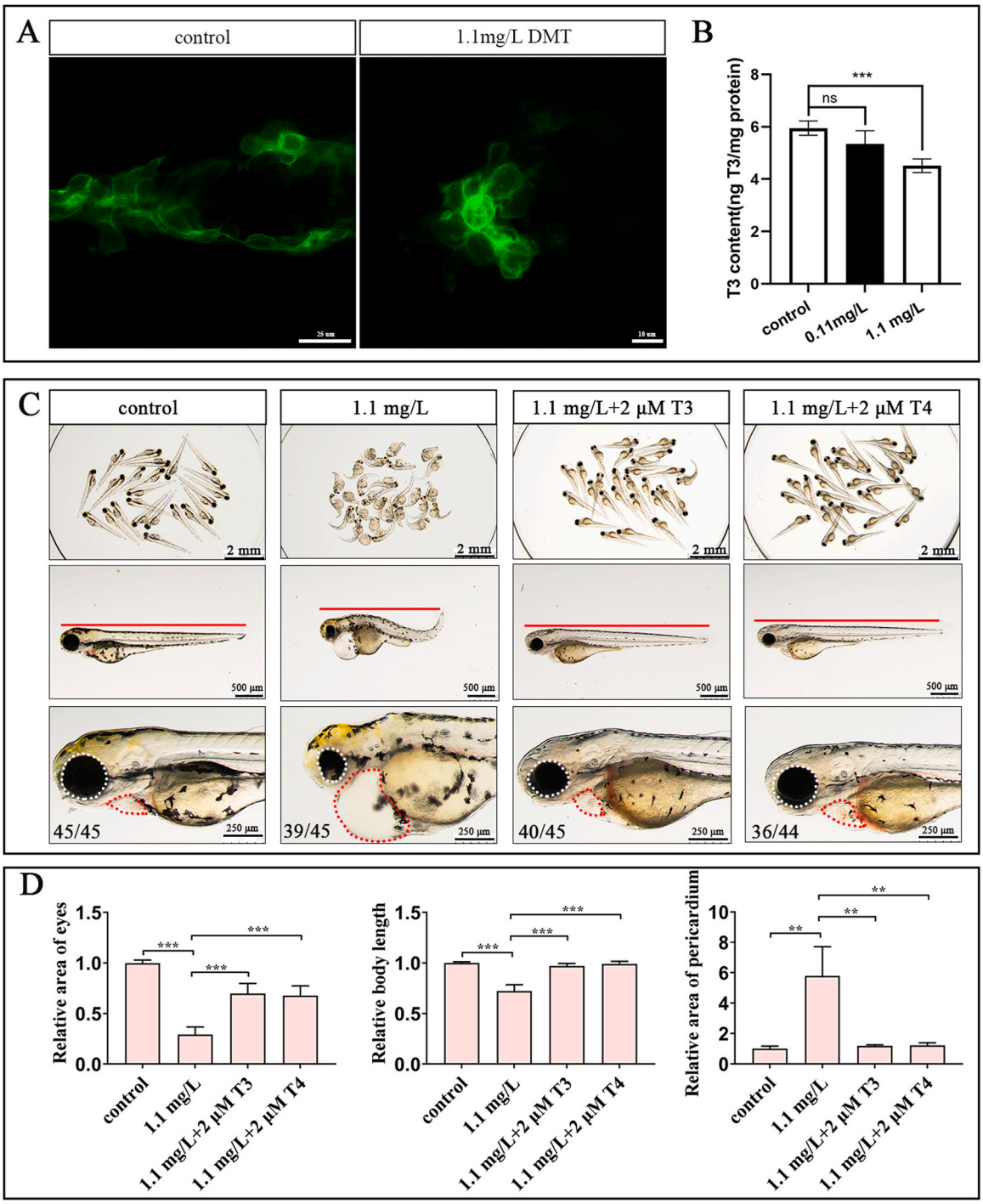

Fig. 6. T3/T4 mitigated the effects of DMT. (A) DMT exposure on the thyroid follicles of zebrafish embryos at 72 hpf. The control group (left) shows normal follicular morphology, while the DMT-treated group (right) exhibits pronounced structural disorganization and enlargement of the follicular cells. (B) The T3 content in embryos decreased after DMT exposure. (C) Representative bright field images of DMT and T3/T4 + DMT treated zebrafish embryos. (D) Statistics of pericardial area, body length, and eye are. The asterisk sign indicates significant differences between DMT treatment and negative control (*p<0.05, **p<0.01, ***p<0.001).

established (Pantos et al., 2008). To investigate whether DMT affects thyroid hormone levels, we utilized the transgenic *Tg(tg:GFP)* line, which labels follicular cells, for dynamic phenotypic analysis of thyroid morphogenesis (Yang et al., 2021b, 2023; Wei et al., 2022). The effects of DMT exposure on thyroid follicle morphology were further examined using confocal microscopy. Zebrafish embryos exposed to 1.1 mg/L DMT for 72 hours exhibited significant structural disorganization in their thyroid follicles compared to the control group. In the control embryos, the thyroid follicles displayed normal, well-organized structures. However, in DMT-treated embryos, the follicles were enlarged and showed irregular morphology. This observation suggests that DMT exposure leads to alterations in thyroid follicle structure (Fig. 6A). Additionally, we measured the changes in T3 levels after DMT exposure. At 0.11 mg/L, DMT caused a slight decrease in T3 levels, whereas at 1.1 mg/L, it significantly reduced T3 levels (Fig. 6B). The rescue experiments were conducted using small-molecule thyroid hormone medications (T3/T4). We assessed several developmental indicators in zebrafish embryos post-rescue, including pericardium area,

body length, and eye area size. The results showed significant improvements: an increase in eye size, longer body length, reduced pericardium size, decreased yolk area, and the embryos exhibited a straight body shape (Fig. 6C, D). These findings suggest that thyroid hormone supplementation effectively rescues the developmental malformations in zebrafish embryos induced by DMT exposure.

4. Discussion

With the continued advancement of modern agriculture, the utilization of pesticides is inevitable and increasing. Extensive literature and investigative reports indicate that the use of pesticides can have significant ecological impacts on various non-target organisms in the environment (Lerro et al., 2021; Moebus and Boedeker, 2021; Park et al., 2020). However, the current understanding of DMT's toxicological effects on non-target species is limited. Most studies focus on the combined toxic effects of DMT with other pesticides, with limited exploration of its standalone mechanisms of toxicity (Fan et al., 2021b). Therefore, in this study, we employed zebrafish as a model organism to assess the embryonic developmental toxicity of DMT on non-target species.

We found that exposure to 0.8 mg/L DMT initiated embryo mortality, while exposure to 1.4 mg/L DMT resulted in 100 % embryo death. The calculated LC50 was approximately 1.0 mg/L. Additionally, exposure to 0.7 mg/L DMT caused a significant reduction in the hatching rate, with 50 % hatching occurring between concentrations of 1.1 and 1.2 mg/L. DMT exposure also led to several developmental abnormalities, including increased atrioventricular spacing, body curvature, reduced heart rate, smaller eye area, shortened body length, as well as pericardial and yolk sac edema. Based on these observations, we conclude that DMT poses developmental toxicity risks to zebrafish embryos. While the concentrations used in this study may exceed those commonly observed in the environment, this approach is essential for exploring the mechanistic aspects of DMT toxicity. Higher concentrations allow for the detection of dose-dependent toxicological effects, revealing the underlying pathways through which DMT impacts zebrafish development.

We observed significant cardiac abnormalities after DMT exposure：atrioventricular spacing of the heart increased significantly，the area of pericardium increased significantly，the heart rate was decreased. Although the zebrafish heart consists of only two chambers, it shares numerous features with the hearts of amniotes, and various cellular and molecular studies highlight their common evolutionary origin (Staudt and Stainier, 2012). *Gata4*, *nkx2.5* and *tbx5a* are important transcription factors for heart morphological development. *Gata4*, *nkx2.5*, *tbx5a* mutations lead to abnormalities in heart structure and function (Mazaud Guittot et al., 2009; Laverriere et al., 1994; Chen et al., 2019; Jiang et al., 2020). Our experiments show that exposure to DMT induces down-regulation of transcription levels of *tbx5a*, *nkx2.5* and *gata4*, which can lead to abnormal heart morphology (looping failure, prolonged distance between the atrium and ventricle). *Myh6* and *vmhc* are expressed specifically in the atrium and ventricle, and their expression patterns subdivide the myocardial precursors into two independent groups (Bakkers, 2011; Yelon et al., 1999; Berdougo et al., 2003). *Myh6* and *vmhc* are significantly down-regulated, which may be related to the various heart defects, as well as pericardial edema and subsequent cell death (Yang et al., 2022b). Upon heart stress, *nppa* is strongly upregulated in the ventricular myocardium (Man et al., 2018). Exposure to DMT triggers upregulation of *nppa*, possibly due to stress caused by DMT to the heart. Therefore, after DMT exposure, the morphology and function of heart development are impaired, which may be related to the disorder of expression of genes related to heart development.

Angiogenesis plays a crucial role in cell proliferation and survival during embryonic development by facilitating oxygen supply (Lee et al., 2021a). Inhibition of *flt1* and *flt4* inhibits angiogenesis in zebrafish embryonic CVP (Lee et al., 2021a). Inhibiting the expression of VEGF and VEGFR2 (*kdr*) will hinder the development of SIV and ISV (Jagadeeshan et al., 2017). In the early development of zebrafish, the yolk sac is the majority of the body, and SIV can effectively absorb nutrients from the yolk and transport them to the embryo (Goi and Childs, 2016). Abnormal retention of the yolk sac will inhibit the nutritional support of the developing organs (Langheinrich, 2003; Pinto et al., 2016; Lee et al., 2021b). Our results show that DMT exposure leads to inhibition of SIV; ISV length shortened, shape defect; DLAV, CVP, CV formation was impaired, and CV was absent in the highest exposure group. This may be due to DMT down-regulation of vascular-related gene expression in zebrafish.

Cell proliferation is one of the most basic processes in biological system, so the quantitative analysis of cell proliferation is very important in many biological applications, such as drug screening, biological agent production and cytotoxicity evaluation (Soobin et al., 2017). In the evaluation of aquatic toxicology with zebrafish as a model animal, the expression of *ccnd1*, *ccne1*, *cdk2* and *cdk6* is often used to evaluate whether drug exposure can affect the normal development of zebrafish. When cell proliferation decreases, the expression of these genes is down-regulated accordingly (Ates et al., 2018; Lee et al., 2020a, 2020b; Schall et al., 2017). Decreased expression of *ccne1* and *cdk2* complexes inhibits G1 transition to S phase, and decreased levels of G0/G1-associated proteins, including *ccnd1* and *cdk6* complexes, lead to inhibited progression of the cell cycle (Cui et al., 2016; Yuan et al., 2015). Our experimental results showed that the expression of these genes related to cell proliferation was significantly down-regulated, and the results of cardiomyocyte antibodies also showed a decrease in cell proliferation. Based on this, we concluded that DMT leads to the decrease of cell proliferation during embryonic development.

Exposure to chemical toxicants increases ROS levels, disrupting the redox homeostasis and leading to oxidative stress (Cheng et al., 2020). The main evaluation indexes commonly used as oxidative stress are ROS level, superoxide dismutase, CAT activity and MDA content (Han et al., 2021; Guo et al., 2019; Yan et al., 2018). The degree of oxidative stress in vivo can be indirectly evaluated by detecting the content of MDA in organisms (Del et al., 2005). CAT is an important member of the antioxidant defense system in almost all aerobic organisms (Gebicka and Krych-Madej, 2019). The expression of *hmox1* responds to oxidative stress (Luo et al., 2022), *nqo1* directly removes superoxide anion free radicals through redox reaction (Lee et al., 2021b; Zhu and Li, 2012). Increased ROS and MDA levels stimulate the activity of antioxidant enzyme CAT and the expression of antioxidant gene *hmox1*, and inhibit the expression of oxidative gene *nqo1*, thus leading to the oxidative stress. Oxidative stress is often associated with disruptions in the development of the heart, vascular system, and cell proliferation (Senoner and Dichtl, 2019; Du et al., 2021), which may be one of the causes of embryonic development defects caused by DMT exposure.

Changes in thyroid status can affect many organs and systems (Wagner et al., 2008). Therefore, it is critical to understand any factors that alter thyroid hormone levels (Babic Leko et al., 2021; van der Spek et al., 2017). Thyroid hormones play a pivotal role in modulating cardiac function, influencing key processes such as heart contractility, rhythm regulation, and vascular integrity (Pantos et al., 2008). Moreover, thyroid hormones are also key regulators of the antioxidant balance (Mancini et al., 2016). We used transgenic zebrafish expressing a fluorescent reporter gene (*Tg(tg:GFP)* line, which labels follicular cells) to evaluate the development of thyroid follicles. Confocal live imaging revealed that DMT exposure leads to structural disorganization in the thyroid follicles. This finding suggests that DMT disrupts normal thyroid follicle development, resulting in altered follicle structure (Yang et al., 2021b, 2023; Wei et al., 2022). Additionally, our analysis of T3 levels in zebrafish exposed to DMT showed revealed a slight decrease in T3 levels at 0.11 mg/L, although this change was not statistically significant. This finding may explain the absence of significant toxicity at 0.11 mg/L, while higher concentrations (1.1Mmg/L) of DMT are capable of exacerbating thyroid-related effects. This decrease in thyroid hormone may

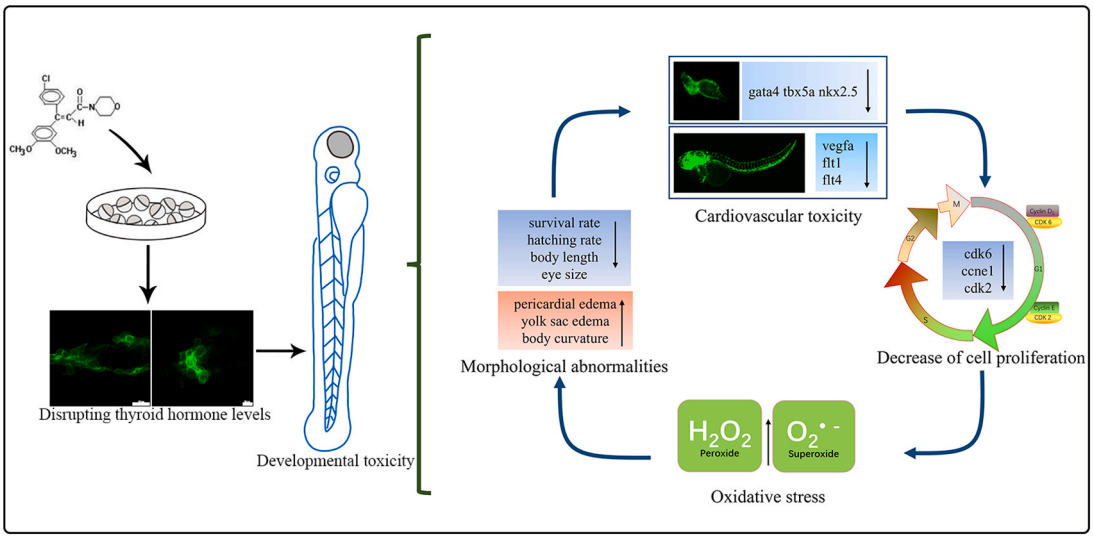

Fig. 7. Schematic diagram of DMT toxicity to zebrafish embryo development. DMT induces oxidative stress in zebrafish embryos by disrupts normal thyroid follicle development, leading to developmental defects of heart and vascular, as well as cell proliferation, thereby leading to an increase in embryonic mortality and abnormalities during zebrafish embryonic development.

indicate that DMT not only affects follicle morphology but also impairs thyroid hormone synthesis or regulation. In response to the observed effects of DMT on thyroid function, we conducted a rescue experiment by adding thyroid hormones in vitro. The goal was to determine if thyroid hormone supplementation could mitigate the DMT-induced toxicity. The results showed partial recovery of the toxic phenotype, suggesting that DMT's effects may involve disruption of thyroid hormone signaling. It remains unclear whether the toxicity of DMT directly targets the thyroid system. Various factors may also interfere with hormone secretion and regulation, leading to endocrine disorders, such as damage to organs like the liver and kidneys, which could also affect the thyroid system (Marty et al., 2018; Wheeler et al., 2013). DMT exposure leads to damage in the follicular cells of zebrafish, affecting thyroid hormone levels and resulting in developmental defects in the heart and blood vessels, as well as deformities in the eyes, body length, and body shape (Fig. 7). Further research is needed to understand how DMT causes disruptions in thyroid hormone regulation.

5. Conclusion

In conclusion, the widespread use of DMT as a pesticide has implications for the ecological safety of nontarget organisms in the environment. We have demonstrated that DMT exhibits significant developmental toxicity in zebrafish, likely leading to developmental defects in the heart and vascular by disrupts normal thyroid follicle development. These findings provide valuable insights for the ecological risk assessment of DMT in environmental

Fundings

This work was supported by the Ministry of Science and Technology of China (2018YFA0801000), National Natural Science Foundation of China (31771606 and 32170853), Natural Science Foundation Project of Jiangxi Province (2018ABC21033).

CRediT authorship contribution statement

Yunlong Meng: Validation, Formal analysis, Data curation. **Kun Jia:** Investigation, Data curation. **Weijian Lu:** Data curation. **Yushan Huang:** Writing – review & editing, Methodology, Formal analysis. **You Wei:** Writing – original draft, Visualization, Software, Investigation. **Huiqiang Lu:** Supervision, Project administration, Conceptualization.

Declaration of Competing Interest

The authors declare that they have no known competing financial interests or personal relationships that could have appeared to influence the work reported in this paper.

Appendix A. Supporting information

Supplementary data associated with this article can be found in the online version at doi:10.1016/j.ecoenv.2024.117413.

Data availability

All the data are in the manuscript

References

Ates, P.S., et al., 2018. Methylparaben induces malformations and alterations on apoptosis, oxidant-antioxidant status, ccnd1 and myca expressions in zebrafish embryos. J. Biochem. Mol. Toxicol. 32 (3), e22036.
Babic Leko, M., et al., 2021. Environmental factors affecting thyroid-stimulating hormone and thyroid hormone levels. Int. J. Mol. Sci. 22 (12).
Baek, S., et al., 2021. Easy and effective analytical method of carbendazim, dimethomorph, and fenoxanil from Protaetia brevitarsis seulensis using LC-MS/MS. PLoS One 16 (10), e0258266.
Bakkers, J., 2011. Zebrafish as a model to study cardiac development and human cardiac disease. Cardiovasc. Res. 91 (2), 279–288.
Bambino, K., Chu, J., 2017. Zebrafish in toxicology and environmental health. Curr. Top. Dev. Biol. 124, 331–367.
Berdougo, E., et al., 2003. Mutation of disrupts atrial function and influences ventricular morphogenesis in zebrafish. Development 130 (24), 6121–6129.
Boberg, J., et al., 2023. Exposure to the pesticides linuron, dimethomorph and imazalil alters steroid hormone profiles and gene expression in developing rat ovaries. Toxicol. Lett. 373, 114–122.
Brown, D.D., 1997. The role of thyroid hormone in zebrafish and axolotl development. Proc. Natl. Acad. Sci. USA 94 (24), 13011–13016.
Chen, L., et al., 2018. Dissipation and residues of fluazinam and dimethomorph in potatoes, potato plants, and soil, determined by QuEChERS ultra-performance liquid chromatography tandem mass spectrometry. Environ. Sci. Pollut. Res. Int. 25 (32), 32783–32790.
Chen, J., et al., 2019. Nkx2.5 insufficiency leads to atrial electrical remodeling through Wnt signaling in HL-1 cells. Exp. Ther. Med. 18 (6), 4631–4636.
Cheng, B., et al., 2020. Effects of spinetoram on the developmental toxicity and immunotoxicity of zebrafish. Fish. Shellfish Immunol. 96, 114–121.
Cui, X., et al., 2016. In vitro toxicological evaluation of ethyl carbamate in human HepG2 cells. Toxicol. Res. 5 (2), 697–702.
Del, R.D., Stewart, A.J., Pellegrini, N., 2005. A review of recent studies on malondialdehyde as toxic molecule and biological marker of oxidative stress. Nutr. Metab. Cardiovasc. Dis. Nmcd 15 (4), 316–328.

Du, Z.C., et al., 2021. Cardiotoxicity induced by Cochinchina momordica seed extract in zebrafish. J. Appl. Toxicol. 41 (8), 1222–1231.
Fan, R., et al., 2021a. Combined developmental toxicity of the pesticides difenoconazole and dimethomorph on embryonic zebrafish. Toxins (Basel) 13 (12).
Fan, R.Q., et al., 2021b. Combined developmental toxicity of the pesticides difenoconazole and dimethomorph on embryonic zebrafish. Toxins 13 (12).
Forhead, A.J., Fowden, A.L., 2014. Thyroid hormones in fetal growth and prepartum maturation. J. Endocrinol. 221 (3), R87–R103.
Gebicka, L., Krych-Madej, J., 2019. The role of catalases in the prevention/promotion of oxidative stress. J. Inorg. Biochem 197, 110699.
Goi, M., Childs, S.J., 2016. Patterning mechanisms of the sub-intestinal venous plexus in zebrafish. Dev. Biol. 409 (1), 114–128.
Guo, Z., et al., 2019. The enrichment and purification of hexabromocyclododecanes and its effects on thyroid in zebrafish. Ecotoxicol. Environ. Saf. 185, 109690.
Han, J., et al., 2021. Dendrobium catenatum Lindl. Water extracts attenuate atherosclerosis. Mediat. Inflamm. 2021, 9951946.
Hao, K., et al., 2019. RNA-seq analysis of the response of plant-pathogenic oomycete phytophthora parasitica to the fungicide dimethomorph. Rev. Argent. Microbiol 51 (3), 268–277.
Hengel, M.J., Shibamoto, T., 2000. Gas chromatographic-mass spectrometric method for the analysis of dimethomorph fungicide in dried hops. J. Agric. Food Chem. 48 (6), 5824.
Hill, A.J., et al., 2005. Zebrafish as a model vertebrate for investigating chemical toxicity. Toxicol. Sci. 86 (1), 6–19.
Horzmann, K.A., Freeman, J.L., 2018. Making waves: new developments in toxicology with the zebrafish. Toxicol. Sci. 163 (1), 5–12.
Jagadeeshan, S., et al., 2017. Toxicity and anti-angiogenicity evaluation of Pak1 inhibitor IPA-3 using zebrafish embryo model. Cell Biol. Toxicol. 33 (1), 41–56.
Jiang, W.F., et al., 2020. A novel TBX5 mutation predisposes to familial cardiac septal defects and atrial fibrillation as well as bicuspid aortic valve. Genet Mol. Biol. 43 (4), e20200142.
Kohler, H.R., Triebskorn, R., 2013. Wildlife ecotoxicology of pesticides: can we track effects to the population level and beyond? Science 341 (6147), 759–765.
Langheinrich, U., 2003. Zebrafish: a new model on the pharmaceutical catwalk. Bioessays 25 (9), 904–912.
Laverriere, A.C., et al., 1994. GATA-4/5/6, a subfamily of three transcription factors transcribed in developing heart and gut. J. Biol. Chem. 269 (37), 23177–23184.
Lee, J.Y., et al., 2021a. Picolinafen exerts developmental toxicity via the suppression of oxidative stress and angiogenesis in zebrafish embryos. Pestic. Biochem. Physiol. 171.
Lee, J.Y., et al., 2021b. Benfuresate induces developmental toxicity in zebrafish larvae by generating apoptosis and pathological modifications. Pestic. Biochem. Physiol. 172.
Lee, J.Y., et al., 2020a. Orbencarb induces lethality and organ malformation in zebrafish embryos during development. Comp. Biochem Physiol. C. Toxicol. Pharm. 233, 108771.
Lee, J.Y., et al., 2020b. Developmental toxicity of chlorpropham induces pathological changes and vascular irregularities in zebrafish embryos. Comp. Biochem Physiol. C. Toxicol. Pharm. 236, 108802.
Lee, W.S., Ham, W., Kim, J., 2021c. Roles of NAD(P)H:quinone oxidoreductase 1 in diverse diseases. Life-Basel 11 (12).
Lerro, C.C., et al., 2021. Pesticide exposure and incident thyroid cancer among male pesticide applicators in agricultural health study. Environ. Int 146, 106187.
Lesmes-Fabian, C., Binder, C.R., 2013. Pesticide flow analysis to assess human exposure in greenhouse flower production in Colombia. Int J. Environ. Res Public Health 10 (4), 1168–1185.
Liang, H., et al., 2011. Dissipation and residue of dimethomorph in pepper and soil under field conditions. Ecotoxicol. Environ. Saf. 74 (5), 1331–1335.
Liu, C., et al., 2012. Behavior of mixed formulation of metalaxyl and dimethomorph in grape and soil under field conditions. Ecotoxicol. Environ. Saf. 84, 112–116.
Li, Y.C., et al., 2022. Comparative transcriptome analysis to investigate the immunotoxicity mechanism triggered by dimethomorph on human jurkat T cell lines. Foods 11 (23).
Luo, K.M., et al., 2022. Zebrafish is necessary for normal development and macrophage migration. Zebrafish 19 (1), 7–17.
Ma, J.Z., et al., 2021. Pyridaben induced cardiotoxicity during the looping stages of zebrafish (Danio rerio) embryos. Aquat. Toxicol. 237.
Mancini, A., et al., 2016. Thyroid hormones, oxidative stress, and inflammation. Mediat. Inflamm. 2016, 6757154.
Man, J., Barnett, P., Christoffels, V.M., 2018. Structure and function of the Nppa-Nppb cluster locus during heart development and disease. Cell Mol. Life Sci. 75 (8), 1435–1444.
Marty, M.S., et al., 2018. Distinguishing between endocrine disruption and non-specific effects on endocrine systems. Regul. Toxicol. Pharm. 99, 142–158.
Mazaud Guittot, S., et al., 2009. Conserved usage of alternative 5′ untranslated exons of the GATA4 gene. PLoS One 4 (12), e8454.
Moebus, S., Boedeker, W., 2021. Case fatality as an indicator for the human toxicity of pesticides-a systematic scoping review on the availability and variability of severity indicators of pesticide poisoning. Int J. Environ. Res Public Health 18 (16).
Munze, R., et al., 2017. Pesticides from wastewater treatment plant effluents affect invertebrate communities. Sci. Total Environ. 599-600, 387–399.
Navarro, I., et al., 2024. Assessing pesticide residues occurrence and risks in water systems: a Pan-European and Argentina perspective. Water Res 254, 121419.
Pantos, C., et al., 2008. Thyroid hormone and myocardial ischaemia. J. Steroid Biochem Mol. Biol. 109 (3-5), 314–322.
Park, A.S., et al., 2020. Prenatal pesticide exposure and childhood leukemia - a California statewide case-control study. Int J. Hyg. Environ. Health 226, 113486.
Pinto, C.L., et al., 2016. Lxr regulates lipid metabolic and visual perception pathways during zebrafish development. Mol. Cell. Endocrinol. 419 (C)), 29–43.
Schall, K.A., et al., 2017. Short bowel syndrome results in increased gene expression associated with proliferation, inflammation, bile acid synthesis and immune system activation: RNA sequencing a zebrafish SBS model. BMC Genom. 18 (1), 23.
Scholze, M., et al., 2020. Quantitative in vitro to in vivo extrapolation (QIVIVE) for predicting reduced anogenital distance produced by anti-androgenic pesticides in a rodent model for male reproductive disorders. Environ. Health Perspect. 128 (11), 117005.
Senoner, T., Dichtl, W., 2019. Oxidative stress in cardiovascular diseases: still a therapeutic target? Nutrients 11 (9).
Siegenthaler, T.B., Hansen, Z.R., 2021. Sensitivity of phytophthora capsici from tennessee to mefenoxam, fluopicolide, oxathiapiprolin, dimethomorph, mandipropamid, and cyazofamid. Plant Dis. 105 (10), 3000–3007.
Soobin, C., et al., 2017. Quantitative analysis of cell proliferation by a dye dilution assay: application to cell lines and cocultures. Cytom. Part A 91 (7), 704–712.
van der Spek, A.H., Fliers, E., Boelen, A., 2017. The classic pathways of thyroid hormone metabolism. Mol. Cell Endocrinol. 458, 29–38.
Staudt, D., Stainier, D., 2012. Uncovering the molecular and cellular mechanisms of heart development using the zebrafish. Annu. Rev. Genet. 46 (46), 397–418.
Wagner, M.S., Wajner, S.M., Maia, A.L., 2008. The role of thyroid hormone in testicular development and function. J. Endocrinol. 199 (3), 351–365.
Wang, C., et al., 2017. Toxicological effects of dimethomorph on soil enzymatic activity and soil earthworm (Eisenia fetida). Chemosphere 169, 316–323.
Wang, S., et al., 2018. Residues, dissipation kinetics, and dietary intake risk assessment of two fungicides in grape and soil. Regul. Toxicol. Pharm. 100, 72–79.
Wang, J.Y., et al., 2022. Human cytochrome P450 3A-mediated two-step oxidation metabolism of dimethomorph: Implications in the mechanism-based enzyme inactivation. Sci. Total Environ. 822, 153585.
Wang, H., et al., 2019. Effects of acetochlor on neurogenesis and behaviour in zebrafish at early developmental stages. Chemosphere 220, 954–964.
Wei, G., et al., 2022. The influence of sunitinib and sorafenib, two tyrosine kinase inhibitors, on development and thyroid system in zebrafish larvae. Chemosphere 308 (Pt 2), 136354.
Wheeler, J.R., et al., 2013. Test concentration setting for fish in vivo endocrine screening assays. Chemosphere 92 (9), 1067–1076.
Xiong, G., et al., 2019a. Immunotoxicity and transcriptome analysis of zebrafish embryos in response to glufosinate-ammonium exposure. Chemosphere 236, 124423.
Xiong, G., et al., 2019b. Clethodim exposure induces developmental immunotoxicity and neurobehavioral dysfunction in zebrafish embryos. Fish. Shellfish Immunol. 86, 549–558.
Xu, X., et al., 2015. A molecularly imprinted polymer for the selective solid-phase extraction of dimethomorph from ginseng samples. J. Chromatogr. B Anal. Technol. Biomed. Life Sci. 988, 182–186.
Xu, Z., et al., 2021. Pesticide multi-residues in Dendrobium officinale Kimura et Migo: method validation, residue levels and dietary exposure risk assessment. Food Chem. 343, 128490.
Yang, L., et al., 2017. Insights into the recognition of dimethomorph by disulfide bridged beta-cyclodextrin and its high selective fluorescence sensing based on indicator displacement assay. Biosens. Bioelectron. 87, 737–744.
Yang, L., et al., 2021a. Dissipation behavior, residue distribution, and dietary risk assessment of fluopimomide and dimethomorph in taro using HPLC-MS/MS. Environ. Sci. Pollut. Res. Int. 28 (32), 43956–43969.
Yang, L., et al., 2022a. A pH- and redox-stimulated responsive hollow mesoporous silica for triggered delivery of fungicides to control downy mildew of Luffa cylindrica. Pest Manag. Sci. 78 (8), 3365–3375.
Yang, R.M., et al., 2021b. Upregulation of GBP1 in thyroid primordium is required for developmental thyroid morphogenesis. Genet Med. 23 (10), 1944–1951.
Yang, L., et al., 2023. Influence of two anti-tumor drugs, pazopanib, and axitinib, on the development and thyroid-axis of zebrafish (Danio rerio) embryos/larvae. Front Endocrinol. (Lausanne) 14, 1204678.
Yang, M.Y., et al., 2022b. Cardiotoxicity of zebrafish induced by 6-benzylaminopurine exposure and its mechanism. Int. J. Mol. Sci. 23 (15).
Yan, Z., et al., 2018. Integrated toxic evaluation of sulfamethazine on zebrafish: including two lifespan stages (embryo-larval and adult) and three exposure periods (exposure, post-exposure and re-exposure). Chemosphere 195, 784–792.
Yelon, D., Horne, S.A., Stainier, D.Y.R., 1999. Restricted expression of cardiac myosin genes reveals regulated aspects of heart tube assembly in zebrafish. Dev. Biol. 214 (1), 23–37.
Yen, P.M., 2001. Physiological and molecular basis of thyroid hormone action. Physiol. Rev. 81 (3), 1097–1142.
Yuan, L., et al., 2015. Resveratrol induces cell cycle arrest via a p53-independent pathway in A549 cells. Mol. Med. Rep. 11 (4), 2459–2464.
Zambito Marsala, R., et al., 2020. First evaluation of pesticides occurrence in groundwater of Tidone Valley, an area with intensive viticulture. Sci. Total Environ. 736, 139730.
Zhong, K., et al., 2021. Effect of flupyradifurone on zebrafish embryonic development. Environ. Pollut. 285, 117323.
Zhu, H., Li, Y.B., 2012. NAD(P)H:quinone oxidoreductase 1 and its potential protective role in cardiovascular diseases and related conditions. Cardiovasc. Toxicol. 12 (1), 39–45.